Methods of long chain branching detection in PE by triple-detector gel permeation chromatography

Thipphaya Pathaweeisariyakul,[1] Kanyanut Narkchamnan,[1] Boonyakeat Thitisuk,[1] Wallace Yau[2]

[1]Siam Cement Group (SCG), SCG Chemicals Co., Ltd., 10 I-1 Road, Map Ta Phut Industrial Estate, Muang District, Rayong Province 21150, Thailand

[2]Polymer Characterization Consultant, USA, www.linkedin.com/pub/wallace-yau

Correspondence to: T. Pathaweeisariyakul (E-mail: thipphap@scg.co.th)

ABSTRACT: Long chain branching (LCB) in polyethylene is one of the key microstructures that controls processing and final properties. Gel permeation chromatography (GPC) with viscometer (IV) and/or light scattering (LS) has been intensely used to quantify LCB. The widespread method to quantify LCB from GPC with IV or LS is the method of LCB frequency (LCB*f*) based on the Zimm–Stockmayer (ZS) random branching model. In this work, the conventional approach was compared with the recently developed method, called gpcBR. The comparison of the sensitivity of both methods is made on highly branched polymer, that is, various grades of commercial LDPE and also on polymer with very low level of LCB, that is, a commercial HDPE with no LCB, converted into several branched test samples of gradually increasing LCB by multiple extrusion. Finally, the linkages of LCB quantities from both methods to the rheological data and processing properties are illustrated. The new gpcBR index can access lower LCB level and shows obviously better relationship with both rheological data and processing properties than LCB*f* from the conventional ZS model. © 2015 Wiley Periodicals, Inc. J. Appl. Polym. Sci. **2015**, *132*, 42222.

INTRODUCTION

In polyethylene technology, long chain branching (LCB) is an important microstructure to control many processing properties, such as melt viscosity, melt strength, die swell ratio, and so forth.[1,2] For example, in LDPE extrusion coating process, LCB structure can improve neck-in properties.[3,4] In pipe technology, high LCB level will change some important properties, such as slow crack growth.[5] Researchers thus attempted to control LCB level occurred in manufacturing process. To support the polymer design development, a well-defined characterization technique for LCB is required. A widespread tool to achieve this approach is gel permeation chromatography (GPC) with high temperature capability, connected with viscosity detector (IV), or light scattering (LS) detector, or both (3D-GPC).[6–10]

The quantification of LCB of polymer by GPC with triple detectors is commonly based on a LCB frequency (LCB*f*) calculation with the assumption of the Zimm–Stockmayer (ZS) random branching model.[6,10,11] In this article from this point on, we will refer this approach as the "current or conventional 3D-GPC method of determining LCB." With the same molecular weight, the root-mean-square radius (R_g) of a branch polymer is smaller than that of a linear polymer. The branching index (g) factor is defined as the ratio of the R_g square of the branched polymer over that of a linear polymer of same molecular weight, as shown in eq. (1). Similarly, the branching index from intrinsic viscosity (g') can also be defined as the ratio of intrinsic viscosity ($[\eta]$) of a branch polymer over the $[\eta]$ of linear polymer of same molecular weight, as shown in eq. (2). These two indices are related with an exponent power ε, so called structure factor, as shown in eq. (3).

$$g = \; <R_g{}^2{}_{\text{branch}}> \; / \; <R_g{}^2{}_{\text{linear}}> \tag{1}$$

$$g' = [\eta]_{\text{branch}} / [\eta]_{\text{linear}} \tag{2}$$

$$g' = g^\varepsilon \tag{3}$$

To estimate g (R_g) from g' ($[\eta]$), a value of this epsilon (ε) parameter must be assumed. The problem is that, this structure factor can vary from 0.5 to 1.5, depending on molecular architecture[9] and recently it was found to be depending on degree of polymerization.[12] It is even more challenging for LDPE which has very complex branching architectures.

From g or g' value, the average LCB per molecule (B) can be estimated from the ZS equation (eq. (4)).

$$g = \frac{6}{B}\left(\frac{1}{2}\left(\frac{2+B}{B} \right)^{1/2} \ln\left(\frac{(2+B)^{1/2}+B^{1/2}}{(2+B)^{1/2}-B^{1/2}} \right) - 1 \right) \quad (4)$$

From the B value obtained from eq. (4), LCBf, a number of LCB per 1000 carbon can be calculated by using eq. (5).

$$\mathrm{LCB}f = \lambda = R \cdot B \cdot \frac{1000}{M} = \text{number of LCB per 1000 carbon} \quad (5)$$

Where, M is molecular weight, and R is a factor of the repeating molecular weight unit. For example, polyethylene, $R = (14 + 14)/2 = 14$, or for PVC, $R = (14 + 13 + 35)/2 = 31$.

A new branching approach, gpcBR, has been recently introduced to analyze LCB by 3D-GPC by Yau and co-workers.[13,14] Comparing to the traditional g or g' and LCBf parameter, this new gpcBR index provides a measure of polymer branching level with a much improved precision, by combining intrinsic viscosity and absolute M_W measurements from viscometer (IV) and LS detectors. The expression of gpcBR is

$$\mathrm{gpcBR} = \left[\left(\frac{K M_{V,CC}^{\alpha}}{[\eta]} \right) \cdot \left(\frac{M_W}{M_{W,CC}} \right)^{\alpha} - 1 \right] = \left[\left(\frac{[\eta]_{CC}}{[\eta]} \right) \cdot \left(\frac{M_W}{M_{W,CC}} \right)^{\alpha} - 1 \right] \quad (6)$$

Where $M_{W,CC}$ and $[\eta]_{CC}$ are the molecular weight and intrinsic viscosity from conventional GPC calculation assuming polymer is linear with no LCB. The $[\eta]$ term is the actual intrinsic viscosity, which is the measured value from the online IV, calculated by the IV peak area method for high precision. M_W is the weight average of absolute molecular weight from LS detector, also calculated by the LS peak area method for high precision. The interpretation of gpcBR is simple and straight forward. For linear polymers, gpcBR will be close to zero. For branched polymers, gpcBR will be higher than zero. In fact, gpcBR value represents the fractional $[\eta]$ change due to the molecular size contraction effect as the result of polymer branching. A gpcBR value of 0.5 or 2.0 would mean a molecular size contraction effect of $[\eta]$ at the level of 50 and 200%, respectively.

The ratio of $[\eta]_{CC}/[\eta]$ or $M_W/M_{W,CC}$ have been used in the literature for measuring polymer LCB, but neither of them by itself can provide good enough precision for practical application. This is because the terms $[\eta]_{CC}$ and $M_{W,CC}$ in the ratio expressions are subjected to variations in experimental conditions of instrument band broadening, elution curve baseline cutting, and variations on the conventional GPC calibration curve itself. This problem of variation in $[\eta]_{CC}$ and $M_{W,CC}$ is however nicely compensated for in the gpcBR formulation (see the right side of eq. (6)), because these two terms appear together in the gpcBR formulation but in the opposite way to cancel out the errors, that is, $[\eta]_{CC}$ being in the numerator and $M_{W,CC}$ being in the denominator. This is the reason to give gpcBR the characteristic of much higher precision than either the $[\eta]$ or M_W ratio. The presence of the ratio of $M_{V,CC}/M_{W,CC}$ in the gpcBR formulation (see the middle portion of eq. (6)) is also helpful in compensating for the molecular weight polydispersity differences among industrial samples. That too helps to provide gpcBR with good precision characteristics.

In this work, the conventional method of LCBf based on ZS model and gpcBR derived from same 3D-GPC data were compared based on the following systems, linear polyethylene, highly branched polyethylene, and polyethylene with very low level of LCB. In addition, both LCB indices from 3D-GPC were related to a simple LCB index from rheological technique and lastly linked to polymer processing property.

EXPERIMENTAL

First of all, a linear sample, SRF1475a (Polyethylene standard) (NIST, USA) was selected to confirm the measurement reliability and create the linear baseline of the LCBf and gpcBR value. For branched polymer, we selected a commercial LDPE as a highly branched polymer (LD-1), and a commercial HDPE with no LCB (HD-1), which is transformed into several branched test samples of gradually increasing LCB by multiple extrusion. LDPE sample was measured 10 times on a high temperature GPC instrument with triple detectors (Polymer Char, Spain): they are IR5 detector, IV, and an 8-angle LS detector (Wyatt Technology, assembled by Polymer Char). The dual IR wavelength capability of the IR5 detector allows the short chain branching (SCB) distribution to be measured across the GPC elution curve. The equipment including control and analysis software was from Polymer Char. This SRF1475a sample was initially used to investigate the sensitivity and precision of the following methods: first is the current LCBf method based on ZS branching model, and second is the recently developed gpcBR method. The second model sample is a linear HDPE, which is passed several times through the twin screw extruder at 200°C, Haake, Germany, to generate LCB from thermal/shear degradation. The samples at even extrusion rounds (2, 4, 6, and 8) were collected and further measured by 3D-GPC.

To link the LCB results from 3D-GPC to rheology and processing properties, different grades of LDPE ranging from low LCB to high LCB content with $M_{W,CC}$ in the range of 100–200K g mol^{-1} were selected. Rheological index used in this report is a simple LCBi parameter, which is the ratio of zero shear viscosity of branched polymer over the linear reference.[15]

To measure with 3D-GPC, the samples were prepared by the following procedure. Around 10–20 pellets were selected and cut into small pieces and weighed around 16 mg (HDPE) and 24 mg (LDPE) in 10-mL vial. The sample vial was then transferred to autosampler of GPC system, and 8 mL of 1,2,4-trichlorobenzene were added into the vial with automatic Nitrogen purging. The sample was dissolved under 160°C for 60 min and 90 min for LDPE and HDPE, respectively. Then the sample solution, 200 μL, was injected into the GPC system with flow rate of 0.5 ml min^{-1} at 145°C in column zone and 160°C in all three detectors. The GPC column temperature was optimized to reduce polymer degradation but still high enough to keep the polymer fully dissolved.

The GPC results were analyzed by "GPC One®" software with additional gpcBR and LCBf calculation from Polymer Char.

To determine zero shear viscosity, the rheometer (DHR3, TA Instrument) with 25 mm parallel plate was used. The creep test was done at 190°C with a constant shear stress of 10 Pa, and
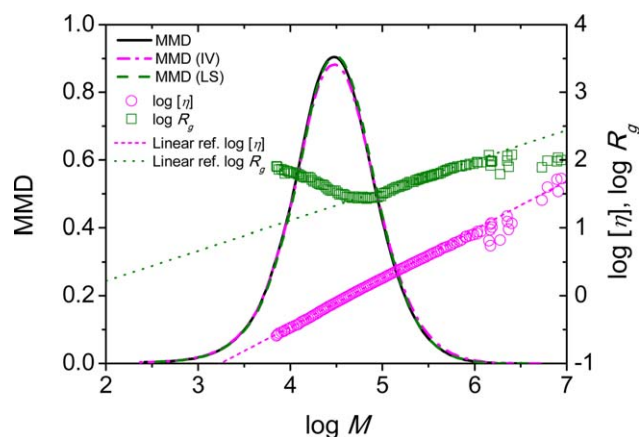
Figure 1. MMD from 3D-GPC with the conformation plot and Mark–Houwink plot of SRF1475a, a linear polyethylene standard. [Color figure can be viewed in the online issue, which is available at wileyonlinelibrary.com.]
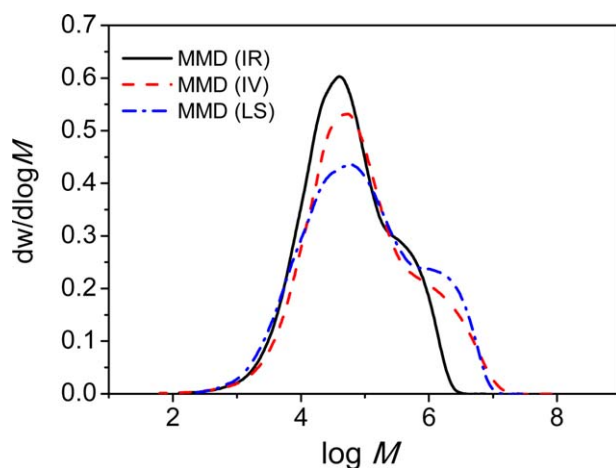

Figure 2. Molecular weight distributions of LD-1 from three detectors. [Color figure can be viewed in the online issue, which is available at wileyonlinelibrary.com.]

the zero shear viscosity was determined at the equilibrium state, where slope of log $J(t)$ versus log (t) was equal to 1; $J(t)$ is creep compliance.

Melt flow index (MI) of processed HDPE was obtained by measuring the rate of extrusion of molten polymer through an orifice at 190°C and 21.6 kg loaded by using melt indexer Model D4002HV (Dynisco). Melt flow rate values were calculated in g/10 min.

RESULTS AND DISCUSSION

Validation of of LCB*f*-ZS and gpcBR Indices on Linear Polymer

The standard linear polyethylene, SRF1475a, has been measured by GPC with online IV and LS. The molar mass distributions (MMD) from three detectors are shown in Figure 1. The conformation plot (Log R_g vs. Log M) and Mark–Houwink plot (Log $[\eta]$ vs. log M) were plotted on the same graph in Figure 1. The averages of gpcBR and LCB*f* values, including intermediate parameters of SRF1475a with standard deviation (STD) from three different measurements are shown in Table I. Figure 1 showed very good agreement in MMD among three online

detectors, IR, IV, and LS. From Table I, it can be seen that all LCB indices, gpcBR, LCB*f* from IV and LCB*f* from LS are very close to zero, indicating linear polymer.
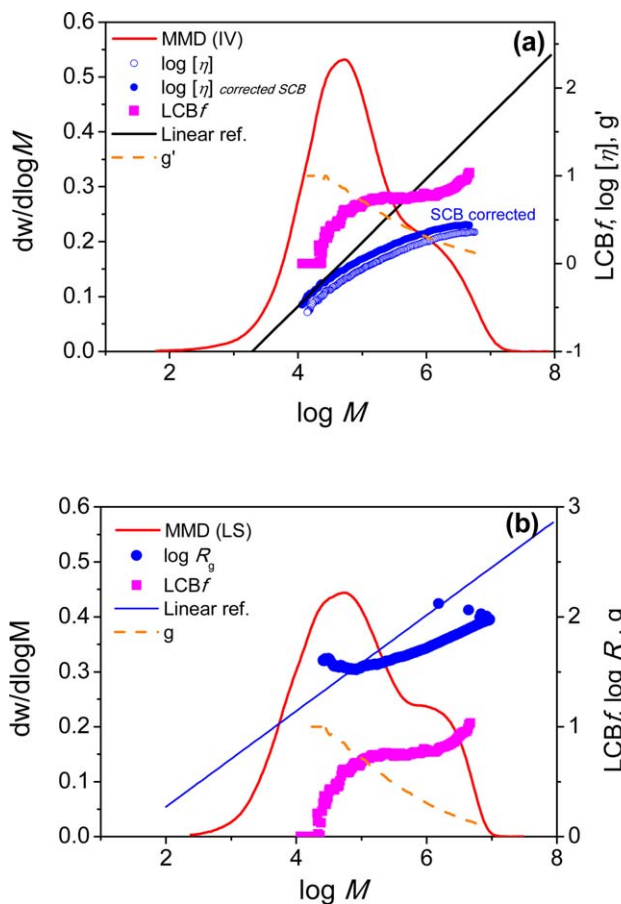

Figure 3. Long chain branching frequency results based on conventional 3D-GPC methods based on ZS branching model (LCB*f*) of LD-1 from (a) viscometer (IV) and (b) light scattering (LS). [Color figure can be viewed in the online issue, which is available at wileyonlinelibrary.com.]

Table I. gpcBR and Intermediate Parameters from GPC Measurement of Linear Polyethylene Standard, SRF1475a

Parameters	Average ± STD
$M_{W,CC}$ (g mol^{-1})	52,666 ± 880
$M_{W,ABS}$ (g mol^{-1})	52,411 ± 1390
$[\eta]_{CC}$ or IV_{CC} (dL g^{-1})	1.04 ± 0.01
$[\eta]$ or IV Bulk (dL g^{-1})	1.01 ± 0.02
$M_{W,ABS}/M_{W,CC}$	1.00 ± 0.02
$[\eta]_{CC}/[\eta]$	1.03 ± 0.01
gpcBR	0.02 ± 0.01
LCB*f* IV	0.006 ± 0.00
LCB*f* LS	0.001 ± 0.00

Table II. Comparison of gpcBR and LCB*f* from IV and LS of LD-1

Parameters	Average ± STD	% Error
Overall gpcBR	4.41 ± 0.08	1.8
LCB*f* (IV) with SCB correction	0.36 ± 0.11	29.3
LCB*f* (IV) without SCB correction	1.60 ± 0.15	9.4
LCB*f* (LS)	0.50 ± 0.04	7.2

Determination of LCB*f* by Conventional 3D-GPC Method Based on ZS Model versus the New gpcBR Method

Determination of LCB*f* and gpcBR. Here a highly branched LDPE, called LD-1, was selected as our test sample, and Figure 2 shows the molecular weight distribution results from three detectors of GPC. As can be seen in the Figure 2, MMD curves from LS and IV of the sample revealed considerable difference from the IR detector, especially at the high-molecular weight region. Accordingly, it appears that the sample should contain long chain branching. Next step is to analyze LCB by using LCB*f* method based on ZS model.

In the conventional 3D-GPC method, LCB*f* results can be analyzed from either IV or LS. Figure 3 presents LCB*f* results from
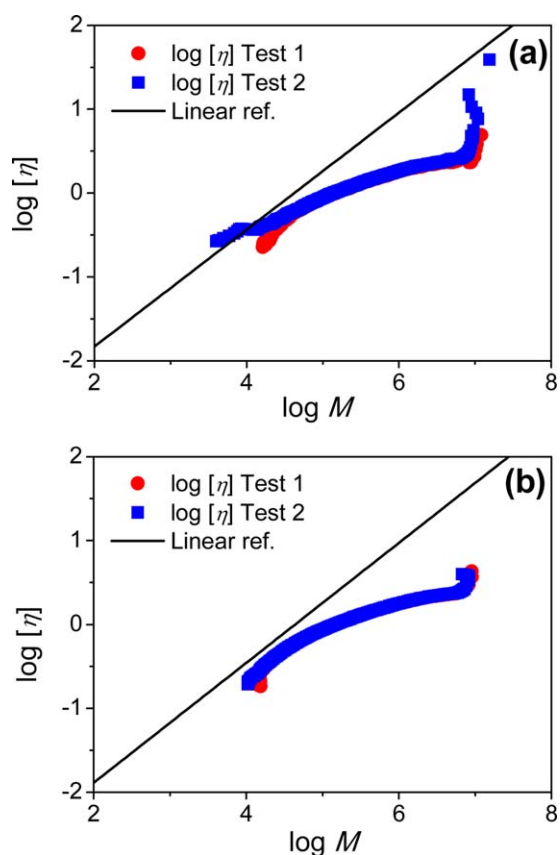

Figure 4. Mark–Houwink plots of two measurements of LD-1 compared with linear reference (a) old viscometer type (capillary bridge viscometer with diluting volume), (b) new viscometer type (capillary bridge viscometer with delay volume). [Color figure can be viewed in the online issue, which is available at wileyonlinelibrary.com.]
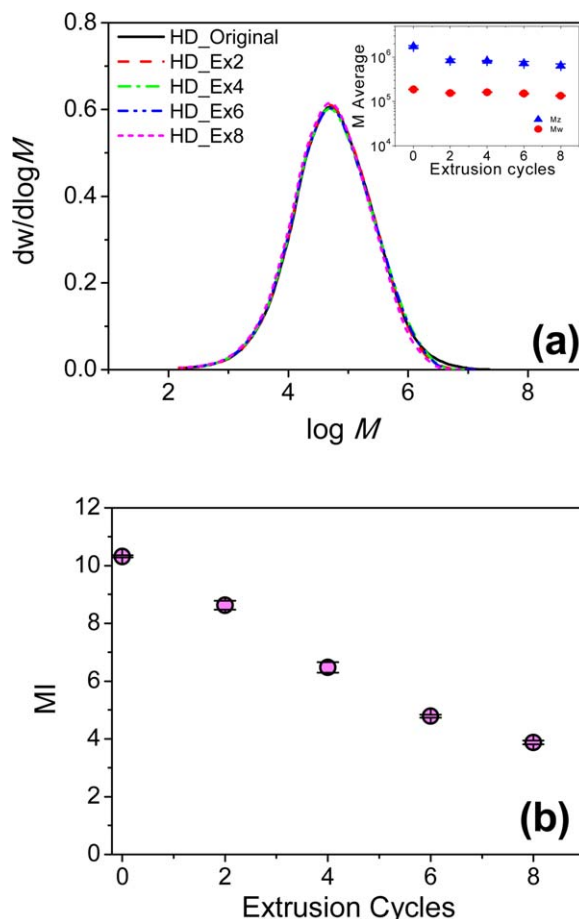

Figure 5. (a) MMD profiles of HDPE with multiple extrusions. Inset: Molecular weight average changing in each extrusion cycles. (b) Melt flow index of multiple extrusion HDPE sample. [Color figure can be viewed in the online issue, which is available at wileyonlinelibrary.com.]

IV (a) and LS (b) of LD-1. The absolute molecular weight and R_g of polymer were determined by 8-angle LS with 2nd order fitted on Debye model,[16] and the calculations were fixed with this method for all measurements.

Consistency of LCB*f* and gpcBR. From the same set of data, gpcBR index can be also calculated by using $M_{W,CC}$ from IR, M_W absolute from LS, $[\eta]_{CC}$ from IR and IV bulk from IV, yielding gpcBR value of around 4.4 for LD-1. From 10 non-consecutive GPC runs, the average results of LCB*f* from IV and LS, and gpcBR of LD-1, and their STDs are tabulated in Table II.

Table II presents that the variations of LCB*f* from either IV or LS show higher values than that of gpcBR. For LCB*f* from IV, the major variation was originated from the adjustment of SCB value to shift the IV curve to touch the linear reference, shown as SCB corrected in Figure 3(a) (see more explanation below). For LCB*f* from LS, the main inconsistency came from the variation in LS calculation ($M_{W,ABS}$), the choice of specific zero-LS angle extrapolation model to calculate M_W and R_g from Zimm plot, and the poor signal to noise detection in low molecular weight region, and so forth.
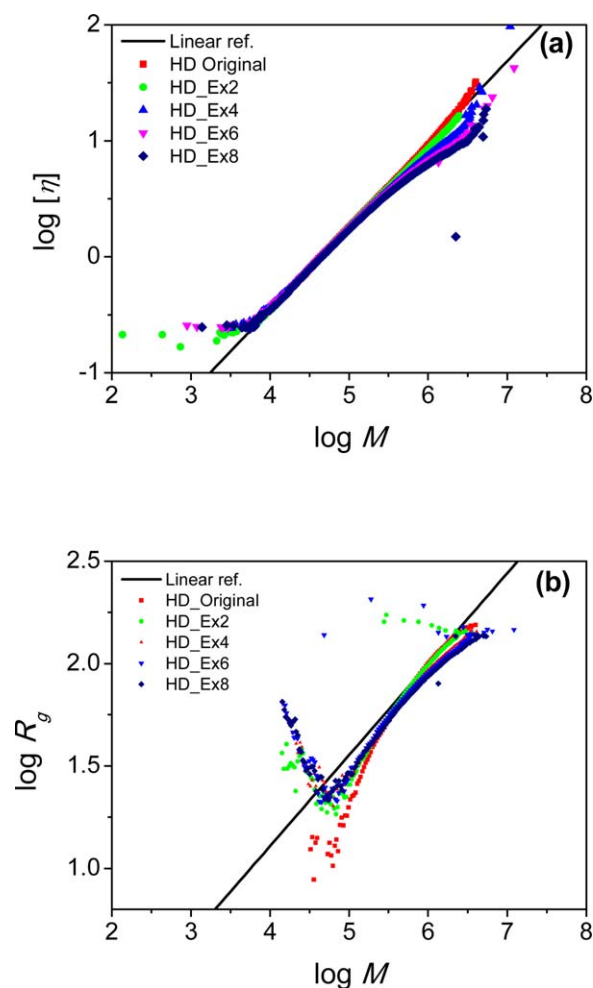
Figure 6. (a) Mark–Houwink and (b) conformation plots from online IV and LS detectors of HDPE with multiple extrusions. [Color figure can be viewed in the online issue, which is available at wileyonlinelibrary.com.]

From the IV data, the *LCBf* can be calculated without SCB correction to give the LCBf average around 1.6 with much less error (reduce from 29.3 to 9.4%).

A parallel shift between the two Log [η] lines in the Mark–Houwink plot is generally considered due to the presence of SCB in the branched sample. Rightly or wrongly, this has been the base for the commonly accepted practice in the GPC field to correct for SCB effect in studying polymer LCB. This correction for the SCB effect can be applied in the commercial GPC software by entering the number of SCBs/1000C to adjust the [η] curve of an unknown sample iteratively until it is superimposed to the low-molecular weight region of the [η] line of linear reference.

Aside from the conventional SCB correction mentioned above, the SCB can be corrected better today with the advent of the new online dual-wavelength IR detector. The short chain branching results can be obtained from the composition calculation when such an IR detector is used. An example of such a result is shown in Figure 3(a).

The sources of error in the conventional method of SCB correction in GPC are from the raw data fluctuation at low-molecular

weight region, as shown in Figure 4(a) for Tests 1 and 2 of repeat injections of a same sample. When the SCB correction was done for these two plots, the data from Test 2 can be shifted to the linear reference with much lower SCB number, resulting in higher LCBf. If the uncorrected data were used and the low-cutoff limit was fixed at log *M* equal to 4.5, both data would yield the same LCBf. However, there were some errors remaining from both fluctuating ends.

To reduce this fluctuation, much better experimental IV signal is needed. The type of IV was changed to be the capillary bridge IV with delay volume (Polymer Char, Spain) which provided more stable baseline and better signal to noise ratio. The previous type was a capillary bridge IV with the diluting volume (Polymer Char, Spain). The LCBf from IV of the new IV for LD-1 provided much less error for corrected and not corrected SCB method, 9.6 and 5.9%, respectively. The curves from the new Type IV are much smoother as shown in Figure 4(b).

Sensitivity of gpcBR and LCBf at Low Level of LCB—The Low LCB Case of the Janzen–Colby Plot[15]

In this part of our study, a linear commercial HDPE was selected and passed through the extruder with multiple cycles to gradually generate LCB in each cycle. Prior to LCB analysis, the molecular weight distribution of five samples, that is, the original sample, plus the 2nd, 4th, 6th, and 8th cycles' samples, are plotted and shown in Figure 5. The MMD of all samples are not significantly different. The weight average molecular weight, M_W, from IR detector of the 2nd to 8th cycles were slightly reduced from that of the original sample, while M_Z of these extruded samples significantly decreased from 1.8×10^6 (original) to 0.6×10^6 g mol^{-1} (the 8th cycle). That means the multiple extrusions affected mostly on the high molecular weight part of the polymer sample.

Interestingly, for multiple extrusion HDPE, the MI decreases with increasing extrusion cycles as shown in Figure 5(b). This decrease in MI, meaning an increase in melt viscosity, would not have been intuitively anticipated in view of the decreasing GPC M_W and M_Z values with increasing extrusion cycles shown in Figure 5(a). Such correlation, however, is exactly what one should expect when low level of LCB is generated during melt
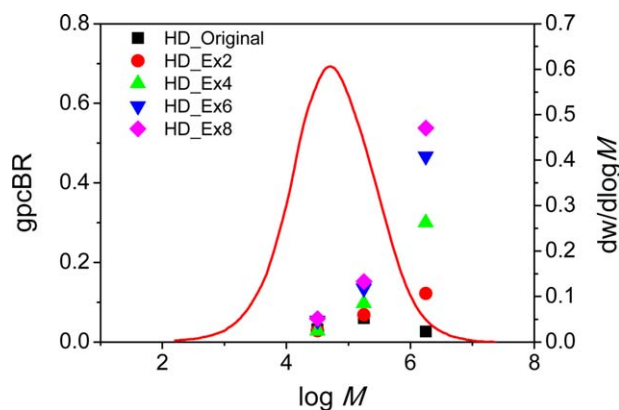

Figure 7. Increment of gpcBR of each molecular weight fraction with extrusion cycles. [Color figure can be viewed in the online issue, which is available at wileyonlinelibrary.com.]
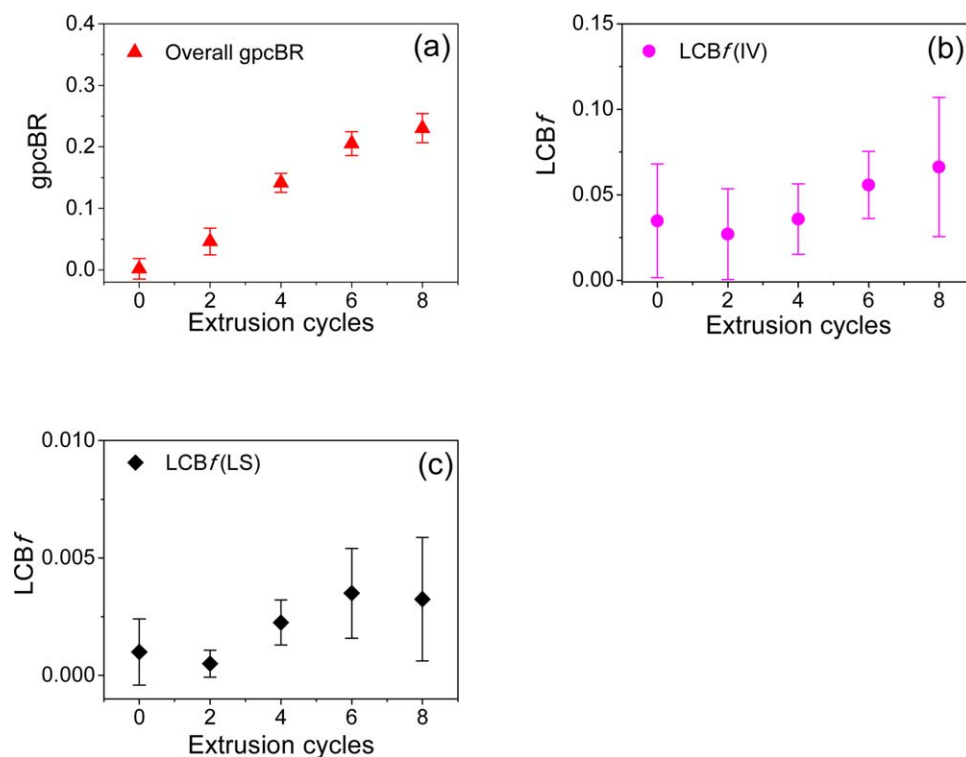
Figure 8. Increasing of LCB; (a) gpcBR, (b) LCBf (IV), and (c) LCBf (LS) of the whole sample with more extrusion cycles. [Color figure can be viewed in the online issue, which is available at wileyonlinelibrary.com.]

extrusion at high temperature, alongside with the concurrent chain-scission processes of the polymer molecules. With the presence of low level of LCB, the melt viscosity of the polymer increases significantly according to Janzen–Colby plot.[15] Furthermore, confirmation of this LCB presence in these samples is provided by the 3D-GPC results discussed below.
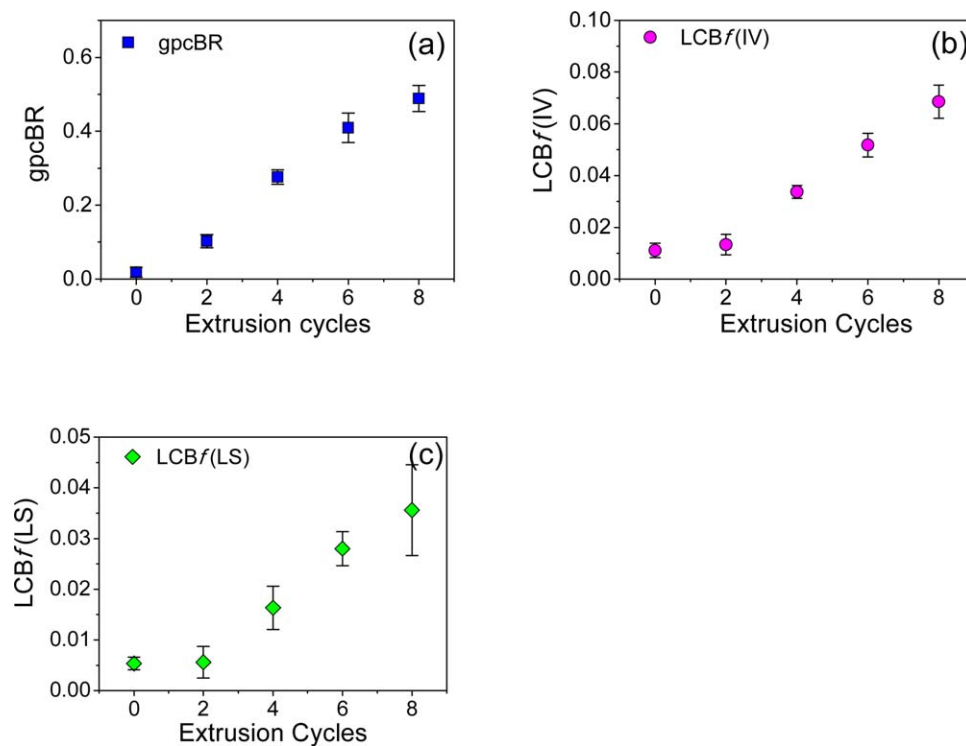

Figure 9. Increasing of LCB; (a) gpcBR, (b) LCBf (IV), and (c) LCBf (LS) at high-molecular weight fraction with more extrusion cycles. [Color figure can be viewed in the online issue, which is available at wileyonlinelibrary.com.]
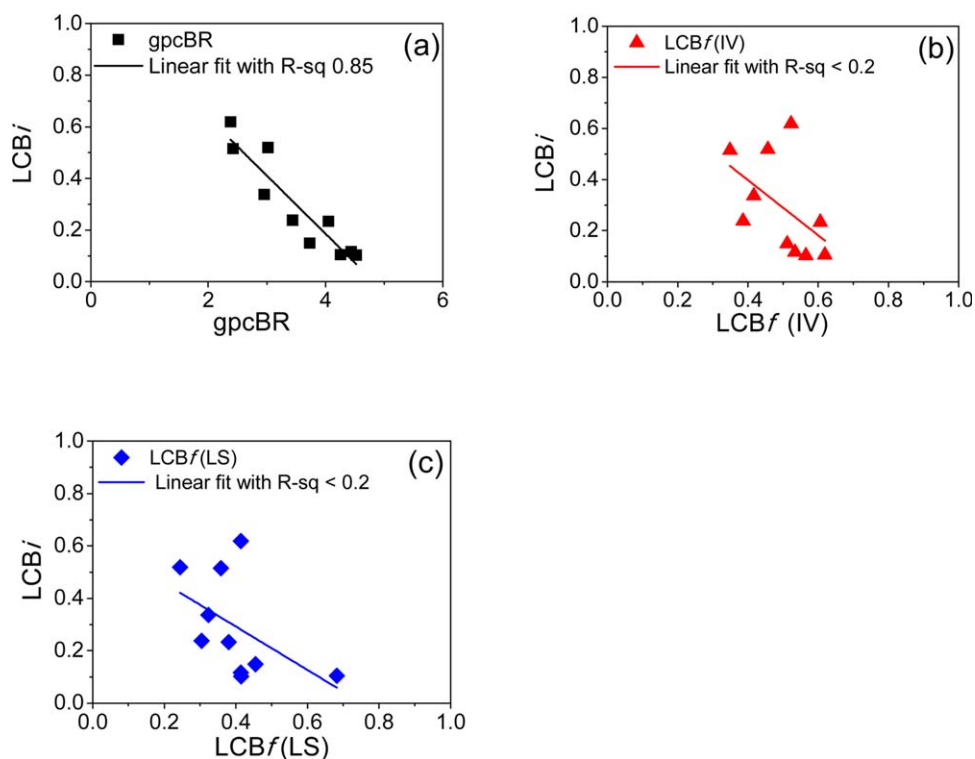
Figure 10. Relationship between LCB*i* and (a) gpcBR, (b) LCB*f* (IV), and (c) LCB*f* (LS). [Color figure can be viewed in the online issue, which is available at wileyonlinelibrary.com.]

From IV and LS online detectors, the Mark–Houwink plot and conformation plot can be obtained. Both plots in Figure 6 show that the more extrusion cycles, the more deviation from linear reference, indicating more LCB.

From 3D-GPC data, gpcBR and LCB*f* can be calculated from IV and LS results. From the option offered in the commercial GPC One® software, gpcBR can be calculated for each of the four separate molecular weight fractions across the sample MWD. Figure 7 shows that gpcBR changed significantly in the highest molecular weight fraction, Fraction 4, among the five test samples, in the exact trend expected of the increasing LCB levels. This can imply that the high-molecular weight polymer gradu-

ally turn into LCB polymer as introduction of heating and shearing in multiple extrusion experiment. The gpcBR values of the first fraction of the test samples were quite noisy and not shown here. This is expected because of the usual limitations of LS and viscosity detection for low-molecular weight polymer.

Likewise, LCB*f* from IV and LS were calculated from 3D-GPC data. To observe the repeatability of these indices, gpcBR, LCB*f* (IV), and LCB*f* (LS) of the original sample and samples from even cycles were tested repeatedly with non-consecutive runs by 3D-GPC. Figure 8(a) illustrates the increasing of LCB with increasing gpcBR of the whole sample with very low deviation. The level of LCB in the starting sample and the second extrusion cycle's sample, and also with the three samples of more extrusion cycles, can be well differentiated. Nevertheless, LCB*f* from both IV and LS cannot definitely distinguish the adjacent cycles, especially for earlier cycles (0 and 2). This experiment shows that gpcBR can access lower level of long chain branch in 3D-GPC with more reliable results than the conventional LCB*f*-ZS method.

With the advantage of GPC technology that offers the ability to access and process data within any molecular weight region of interest, the LCB indices can be determined in selected regions. In this study, since LCB was expected to be generated mostly in the high molecular weight region, therefore, the gpcBR and LCB*f* in this fraction were calculated and re-plotted here versus the number of extrusion cycles in Figure 9. The gpcBR results at high-molecular weight region [blue squares in Figure 9(a)] can even more clearly separate all test samples apart, as compared with Figure 8(a) for the whole sample. Remarkably, thanks to the GPC advantage of focusing only on the high-
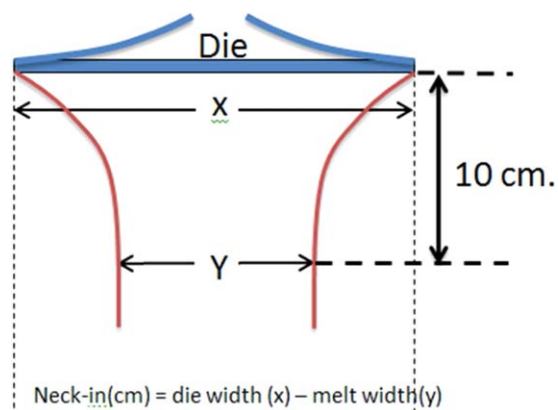

Figure 11. Schematic drawing of Neck-in measurement in extrusion coating process. [Color figure can be viewed in the online issue, which is available at wileyonlinelibrary.com.]
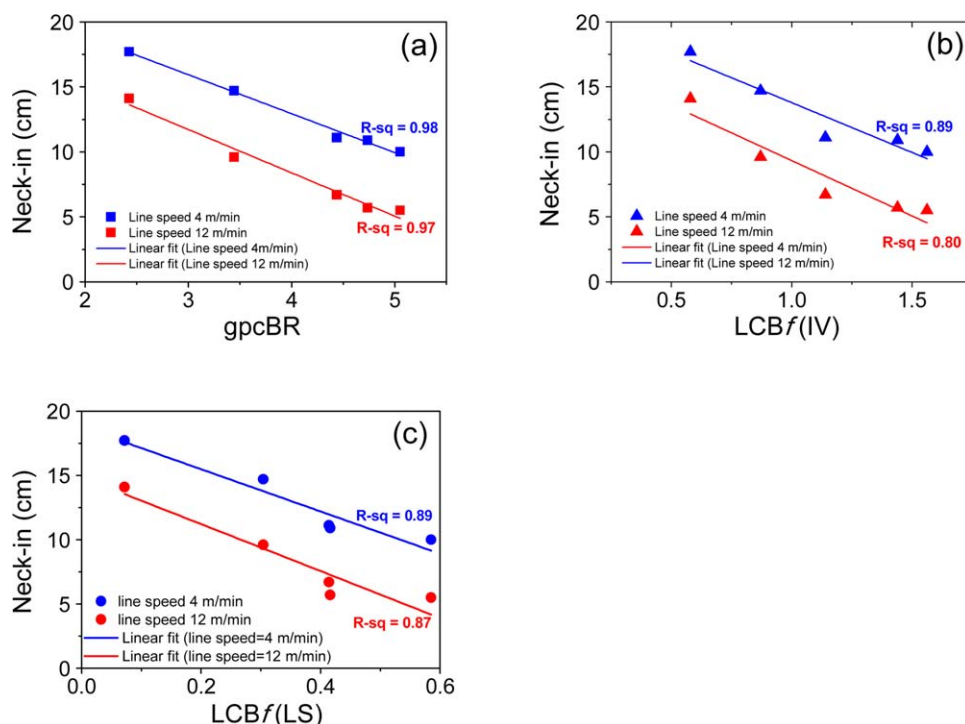
Figure 12. Long chain branching and neck-in relationship (a) gpcBR, (b) LCBf (IV), and (c) LCBf (LS). [Color figure can be viewed in the online issue, which is available at wileyonlinelibrary.com.]

molecular weight region, even the variation of LCBf from both IV and LS detector were also now significantly improved. Nevertheless, the LCBf of the 2nd cycle sample was still unable to be differentiated from the original sample.

Comparison of LCB from 3D-GPC and Rheology—The High LCB Case of the Janzen–Colby Plot[15]
Besides 3D-GPC, another widely used method to determine LCB is rheology.[15,17–19] Here, the comparison between the LCB from 3D-GPC and the rheology was reported. The rheology LCB index, called LCBi, is defined in the following equation.

$$LCBi = \frac{\eta_{0,branch}}{\eta_{0,linear}} \qquad (7)$$

where $\eta_{0,branch}$ is the measured zero shear viscosity of the branched sample, and $\eta_{0,linear}$ is the zero shear viscosity of the linear polymer which has same GPC measured backbone $M_{W,CC}$ as the branched polymer, calculated from $\eta_0 = 2.29 \times 10^{-15} M_W^{3.65}$.[20]

In this part, the relationships between rheology LCBi and the LCB measurement from 3D-GPC, that is, gpcBR, LCBf (IV), and LCBf (LS) were illustrated. This test was done on the same set of LDPE samples used in "Polymer structure property relationship—relationship of LCB and processing properties" below for the coating neck-in test. The plot between gpcBR and LCBi shown in Figure 10(a) provided the best linear fit. Although LCBf from both IV and LS in Figure 10(b and c), respectively, shows poor correlation with LCBi, they provide the same trend as gpcBR that is LCBi decreases with increasing LCB from 3D-GPC. This trend of decreasing LCBi with increasing LCB for LDPE is the expected result according to the well-known Janzen–Colby plot of predicting LCB effect on rheology for polymers with very high level of LCB.[15]

But, due to the excessive scattering of the LCBi plot versus LCBf data, the predictability of melt viscosity property of polymer sample from GPC-LCBf measurement is practically all lost, non-existing any more for all practical considerations. This has been the problem commonly faced in studies attempting to establish correlation of GPC determined LCB results with polymer rheological properties. The use of gpcBR suggested in this work should help to provide an improvement in such studies in the future.

Knowing the high precision value of the gpcBR results as demonstrated in "Sensitivity of gpcBR and LCBf at low level of Long chain branching—The low LCB case of the Janzen-Colby plot" above on the HDPE extrusion study, the most of the scatter of the data points in Figure 10(a) could be caused more significantly from the variations in the LCBi measurement than that from gpcBR.

Polymer Structure Property Relationship—Relationship of LCB and Processing Properties
LCB is one of the most important microstructures that influences the processing properties, especially on Neck-in level.[3,4] In this part of our study, various grades of LDPE have been selected to verify the relationship between Neck-in and LCB. The processing test was investigated by using a laboratory extrusion coating (Collin, Germany) with fixing line speed of 4 and 12 m min^{-1}. The neck-in value was measured at the distance of 10 cm from die lip as a difference between the melt width and the die width as shown in Figure 11.

Figure 12(a) presents the linear relationship between Neck-in and gpcBR with R-square greater than 0.97. Neck-in value is reduced with higher gpcBR, which represents higher long chain

branching. Low neck-in value indicates good processing performance. Similarly the LCBf from IV and LS also shows linear relationship with Neck-in as shown in Figure 12(b,c), but with lower R-square than gpcBR where both results of gpcBR and LCBf values are calculated from exactly the same set of data files.

CONCLUSIONS

GPC with online IV and LS detector is an effective tool to determine LCB ranging from very low to very high level. The gpcBR method provides more reliable results than the method of LCBf based on ZS model. This is shown in the experiment with slightly increasing LCB in HDPE with multiple extrusion cycles. We showed here that gpcBR can access lower LCB level than the current LCBf approach with results calculated from the same experimental data files, (under exactly the same instrumental and measurement conditions). Moreover, the gpcBR results showed a nice correlation to the rheological LCBi measurement, and also to the processing properties, such as the neck-in data in LDPE coating process, with higher r-square correlation index value than that of the LCBf results.

REFERENCES

1. Barroso, V. C.; Maia, J. M. *Polym. Eng. Sci.* **2005**, *45*, 984.
2. Yan, D.; Wang, W.-J.; Zhu, S. *Polymer* **1999**, *40*, 1737.
3. Honkanen, A.; Bergström, C.; Laiho, E. *Polym. Eng. Sci.* **1978**, *18*, 985.
4. Kouda, S. *Polym. Eng. Sci.* **2008**, *48*, 1094.
5. Mehta, S. D.; Reinking, M. K.; Joseph, S.; Garrison, P. J.; Lewis, E. O.; Schwab, T. J.; Yau, W. W. Pub. No. US2009/0304966, United State, **2009**.
6. Grcev, S.; Schoenmakers, P.; Iedema, P. *Polymer* **2004**, *45*, 39.
7. Stadler, F. J. *Rheol. Acta* **2012**, *51*, 821.
8. Suarez, I.; Coto, B. *Eur. Polym. J.* **2013**, *49*, 492.
9. Tackx, P.; Tacx, J. C. J. F. *Polymer* **1998**, *39*, 3109.
10. Yu, Y.; DesLauriers, P. J.; Rohlfing, D. C. *Polymer* **2005**, *46*, 5165.
11. Zimm, B. H.; Stockmayer, W. H. J. *J. Chem. Phys.* **1949**, *17*, 1301.
12. Kratochvíl, P.; Netopilík, M. *Eur. Polym. J.* **2014**, *51*, 177.
13. Enos, C. T.; Rufener, K.; Merrick-Mack, J.; Yau, W. Water International GPC Symposium Proceedings, Baltimore, MD, 6–12 Jun **2013**; 2003.
14. Enos, C. T.; Yau, W. PITTCON (Pittsburgh Conference) 2004 preceeding, Chicago, IL, **2004**.
15. Janzen, J.; Colby, R. H. *J. Mol. Struct.* **1999**, *485*, 569.
16. Podzimek, S. Light Scattering, Size Exclusion Chromatography and Asymmetric Flow Field Flow Fractionation—Powerful Tools for the Characterization of Polymers, Proteins; Nanoparticles; Wiley: Hoboken, New Jersey, **2011**.
17. Wood-Adams, P. M.; Dealy, J. M.; deGroot, A. W.; Redwine, O. D. *Macromolecules* **2000**, *33*, 7489.
18. Larson, R. G. *Macromolecules* **2001**, *34*, 4556.
19. Stadler, F. J.; Karimkhani, V. *Macromolecules* **2011**, *44*, 5401.
20. Karjala, T. P.; Sammler, R. L.; Mangnus, M. A.; Hazlitt, L. G.; Johnson, M. S.; Hagen, J. C. M.; Huang, J. W. L.; Reichek, Detection of low levels of long-chain branching in polyolefins. K. N. ANTEC 2008 preceeding, **2008**, p. 887.